International Journal of Engineering Trends and Technology
ISSN: 2231–5381 / https://doi.org/10.14445/22315381/IJETT-V71I4P227

Volume 71 Issue 4, 309-322, April 2023

Original Article

Boosting a Regular Bicycle into a Low-cost E-bike for Public Urban Transportation

Victor Huatuco-Villena[1], Julio Motta-Claudio[2], Pedro Portillo-Mendoza[3], Carlos Sotomayor-Beltran[4]

[1,2,3,4]*Universidad Tecnológica del Perú, Lima, Perú*

[3]*Corresponding Author: c16985@utp.edu.pe*

Received: 25 February 2023 Revised: 02 April 2023 Accepted: 12 April 2023 Published: 25 April 2023

Abstract *- The present work has the purpose of determining and implementing the optimal design to convert a conventional bicycle into an electric bicycle (e-bike) for public transport in order to help people to move around urban areas. The proposed e-bike is also affordable and meets the required standards and regulations. The design of the e-bike was carried out based on the mathematical model of a regular bicycle with the parameters for urban transport for its conversion into an electric bicycle. From this, the selection of components, mechanical upgrades, hardware and firmware designs was carried out. Finally, a data acquisition method for the tests was conducted. The results of the design parameters, the maximum motor assistance speed, the inclination control and the results against different slopes were obtained from these tests. Our results showed that, based on the incorporated control system, the necessary standards and regulations were met, hence, putting forward a low-cost e-bike as an alternative to public urban transportation.*

Keywords *- Electric bicycle (e-bike), Regular bicycle, Transportation, Brushless motor, Mathematical model.*

1. Introduction

In the current national context, public urban transportation is one of the main problems citizens face every day. As [1] argues, the deficiency of the urban transportation system affects the economy, negatively impacts the industry's growth, generates losses in the private sector due to the costs of mobilizing its workers and, more importantly, affects the condition of lives of people. For this reason, people choose to look for other means of transport to cover their needs.

On the one hand, the most considered option is acquiring a combustion engine vehicle for personal use to transport people. However, this option involves high costs in acquiring and maintaining the vehicle due to the high prices of fossil fuels. On the other hand, another option is the acquisition of a personal non-motorized vehicle, such as a bicycle or some type of scooter, but this supposes overexertion for users who are not physically active. So, the optimal and most popular solution would be the acquisition of an electric vehicle to be able to get around the city; however, this new technology, which is still in its early years, is very expensive and not very affordable for people who mostly use public transportation.

To buy an electric bicycle (e-bike), as [2] mentions, has the main advantage in the layout of its parts because it provides greater security and performance to the user by having a layout designed and calculated in its development. However, it has the disadvantage of a high cost, which is why users search for a cheaper option, which is to purchase a conversion kit from a conventional bicycle to an electric one.

The main advances in electric vehicles for personal transport are focused on developing e-bikes, which are regular bicycles powered by an electric motor powered by a battery. Within these advances, developments such as [3, 4] are presented, which are very similar in terms of the selection of the most crucial components for the development of e-bikes, such as the motor, the battery and its controllers. However, the technologies of these components find variations according to characteristics that are sought to be highlighted in a particular way.

The selection of the motor is a very critical process since, as stated by [3, 5], it is necessary to take into account the forces involved in the movement of the cyclist-bicycle set, which is subject to the forces of resistance, wind resistance, slope resistance, and ground resistance. These engine considerations are very necessary to optimize resources and generate maximum efficiency in the power and speed that the engine can supply.

On the one hand, [3] mentions the importance of implementing a brushless motor (brushless motor) or hub-type motor to generate the system's movement since these

motors are very efficient in supplying the necessary torque and the speed they reach. They can favour displacement; this is also supported by [6, 7, 8, 9, 10]. Likewise, as [4, 6, 7] maintain, implementing the motors in question does not imply some type of structural modification of the bicycle frame since this motor is fixed to the axle on the wheel, front or front or rear. On the other hand, [4] maintains that it is necessary to have a central type motor coupled to the pedal in order to generate the necessary thrust to move the bicycle.

In reference to the selection of batteries for the operation of the e-bike, it is a point of debate since a consensus is not achieved between technologies of assisted bicycles. In the first place, [3] argues that the most suitable battery for the purposes of feeding the bicycle must be Lithium-Phosphate due to the energy density (Wh/kg) that it can provide to the system due to the life cycles or charge. For the useful life, it has in contrast to batteries with similar technologies such as Lithium-Cobalt or Lithium-Magnesium. Secondly, [6] argues that the most appropriate batteries are solid acid batteries (Lead Acid Batteries);. However, this type of battery is less energetically dense than the batteries used by [3]; these batteries are just as safe and allow them to be loaded and worn with less worry in life cycles. Likewise, [27] also maintains that solid-acid batteries are the most suitable for e-bikes; however, it is a bit more specific than [3] since it is argued that sealed lead-acid batteries are the best.

The different components of the aforementioned developments are the most critical to deal with due to their physical characteristics. From this point, the motor speed control system that supports [3] and the SPV system that supports [6] do not generate a greater physical impact within the mechanical characteristics of the bicycle since they have a reduced weight.On the other hand, thes e components' electronic and control implications are paramount within the study system. First, as [3, 6, 7, 11, 12, 13] argue, considering a brushless motor requires a particular control system, which is the electronic speed controller (ESC), since this motor has 3 wires: 2 for power and one to sense the rotor position and toggle power and sense wire configuration. This system will be in charge of controlling the speed of the motor during its operation. Second, as [4, 14, 15] argue, it is a simpler control system since the central motor is a two-wire DC motor for power supply. This means the control can be by pulse width modulation or ON-OFF control.

In view of the above, the option of transforming conventional bicycles into electric bicycles with an optimal design that helps in moving around urban areas, that is affordable, that meets the necessary standards and that follows the respective regulations is considered in this work. Thus, the optimal design is proposed to convert a conventional bicycle into a low-cost e-bike for urban transportation from a mechanical design and an electronic design. Tests were carried out to improve the bicycle's performance and also for the user's safety.

2. Methodology

2.1. Mathematical modelling

As the first step in this research project's methodology, the mathematical modeling of G. The jasree and R. Maniyeri on a conventional bicycle [16] was used, given its similarity with the physical behavior of the bicycle used for this work. From the model, the main characteristics of the moving system, such as torque and, especially, power, were determined.

2.1.1. Torque Determination

In equation 1, the torque formula is provided. For this, it was necessary to obtain the forces dependent on the user's physical characteristics and the topological characteristics of the terrain through which they move.

$$Tmotor = r\left(M\frac{\partial v}{\partial t} + Fw + Frr + Fa\right) - Tuser \quad (1)$$

Fw is the aerodynamic drag force. To calculate this force, the values of the reference area of the cyclist-bicycle system and the aerodynamic drag coefficient were taken from [17] since this source is a reference when studying fluid mechanics. Frr is the rolling resistance force or forward resistance force. To determine the mass of the system, the information provided by [18] will be used, which indicates that the average mass of a Latin American person is around 67.7 kg; this will be taken as an approximate value of the average weight of the inhabitants of the area urban area in the city of Lima. Likewise, the average mass of a bicycle will have to be added, which is between 7.5-9 kg, so that an average value will be taken for the purposesof this study; that is, the mass of the bicycle will be 8.25 kg. Therefore, the system's mass will be equal to 75.95 kg and considering that it carries an additional charge, the mass of the resulting system will be 90 kg. The slope of the terrain and the characteristics of the area on which the e-bike will travel must be considered. Therefore, as [19] maintains, for places with flat terrain, the minimum slope must be 0.5% and must not exceed 10%, considering 100% as 90°. Fa is the gradient resistance force. For this is needed the total mass of the system, gravity and steepness of the slope is. To estimate the rider's torque (*Tuser)*, we focus on what was presented by [19, 20], who present a graphical representationof the development of torque generated by a cyclist as a function of time; this is necessary since it has to be taken into account to calculate the necessary torque to be complemented by the electric motor. The block diagram presented in Figure 1 (developed in Simulink) will be responsible for generating the graphical representation of the pedaling of the person as a function of time. This block

diagram will provide the signal that will be used to input the rider's torque signal. This is important for the rider's torque, as it must be subtracted from the overall torque to determine the motor's torque.

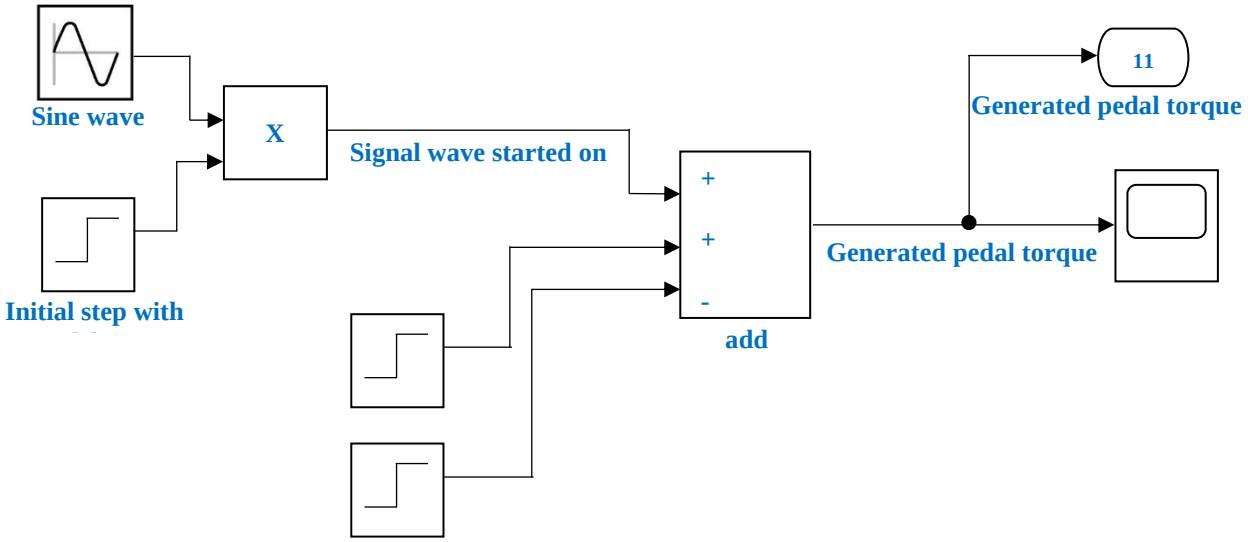

Fig. 1 Block diagram of the torque generator for the user

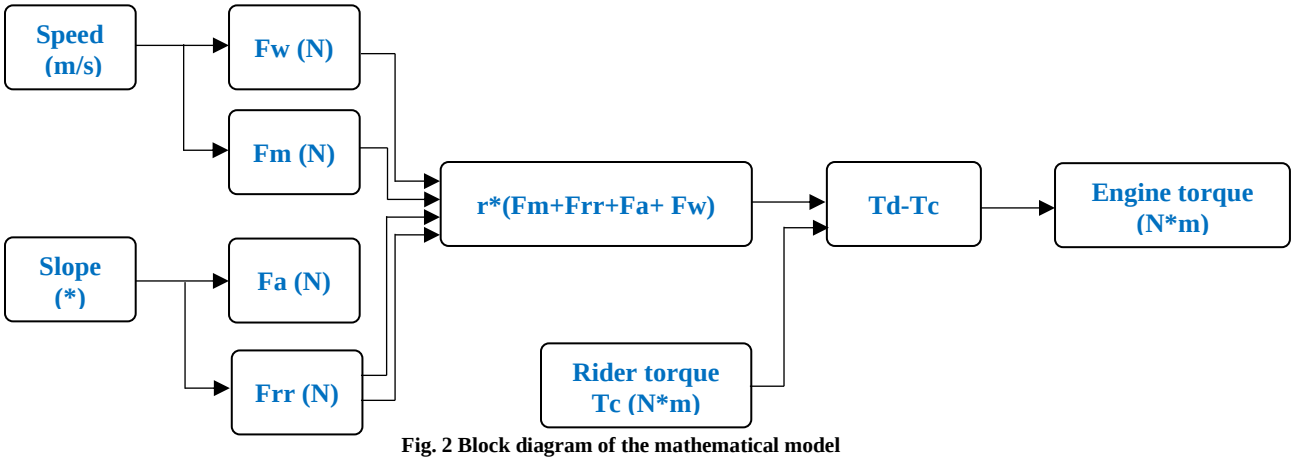

Fig. 2 Block diagram of the mathematical model

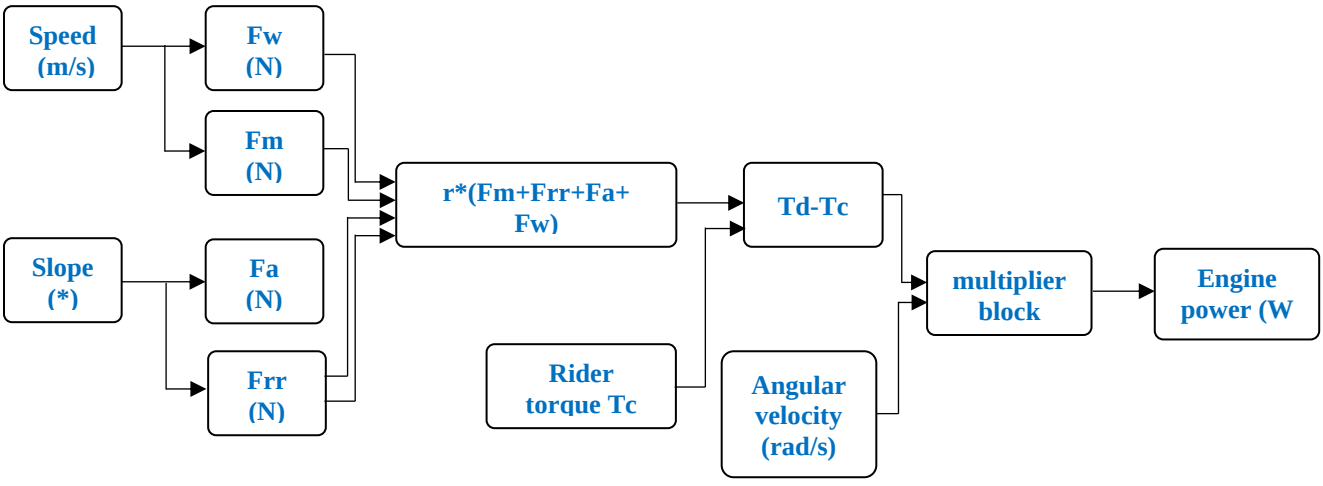

Fig. 3 Block diagram for the engine power calculation

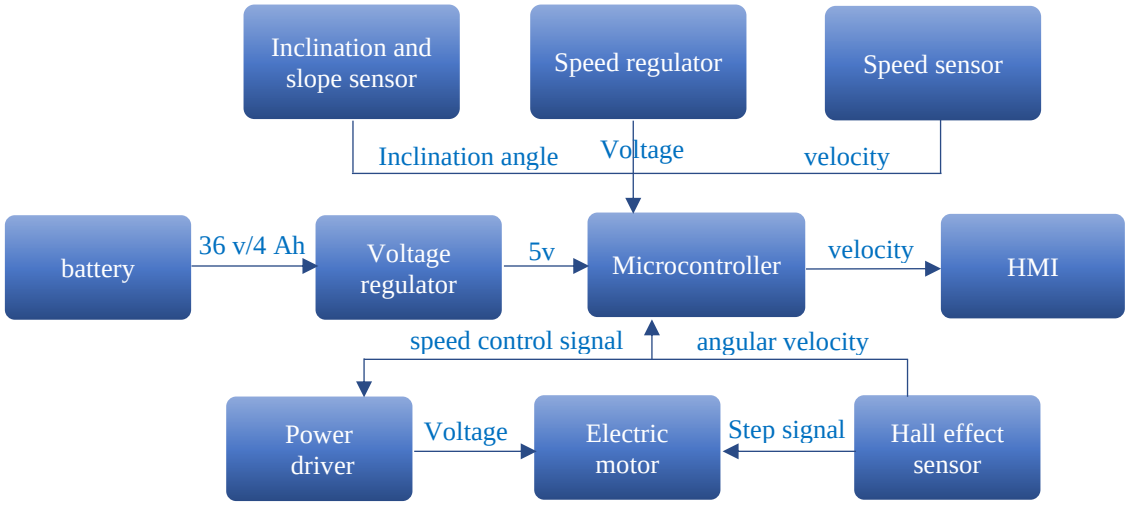

Fig. 4 System block diagram

Once all the variables are established, equation 1 will be represented as a block diagram because it represents the motor torque (Tmotor) necessary to generate a certain speed at a certain slope, depending on the pedalling of the person. In Figure 2, it can be seen that the recreated Simulink block diagram was used to determine the motor torque necessary to generate the system's movement. Likewise, the system's inputs are observed: the slope of the route and the speed at which the cyclist moves.

2.1.2. Determination of Engine Power

Once having determined the necessary torque for the assistance generated by the motor, we proceed to calculate the power that is generated by it during its journey. This is calculated using Equation 2.

$$Pwatt = TmotorWmotor \quad (2)$$

Where *Pwatt* is the power in watts of the motor, *Tmotor* is the engine torque, and *Wmotor* is the angular velocity of the motor wheel of the bicycle. In Figure 3, we can see the Simulink block diagram to calculate the engine power.

2.2. Block Diagram of the Proposed Hardware

Once the motor power necessary to generate the movement of the bicycle and the cyclist has been calculated, it was necessary to consider the components of the electric bicycle, presented in Figure 4, in which their interconnections are observed to guarantee the operation of the system.

First, it is observed that the system requires a battery to power the system. This battery must have the necessary capacity to power both the control and power parts.

Second, it is observed that the addition of a microcontroller was considered to carry out the control actions necessary for the system's operation; this microcontroller would have toguarantee the ability to read and generate analog signals and have implemented the basic communication protocols, I2C, SPI and UART. Likewise, the implementation of sensors that help to control the system was considered; for this, the need for a sensor that measures the angles of inclination in ordered axes was crucial in order to perform situational control of the engine and follow the established regulations indicated in [21] and supported by [22]. In addition, the implementation of a speed controller was considered that would allow the user to regulate the speed at which it moves, and, in the same way, a speed sensor was implemented, which would help control the speed of movement of the system. Third, it was considered to implement an HMI screen to be able to interactively visualize the characteristics of the displacement of the system and observe the parameters to be taken into consideration. Finally, it was considered that implementing the power driver for the motor and the Hall effect sensors depended directly on the selection and implementation of the motor.

2.3. Selection of Components

2.3.1 Motor Selection

For the selection of the electric motor, the maximum power necessary to guarantee the movement was taken into account, as well as the limit power that this device must have to comply with the regulations established by [22]. The maximum power calculated from the mathematical modelling will be taken, which was 275 Watts. On the other hand, as mentioned, the maximum power allowed by law and supported by [22], 350 Watts, will be respected. Therefore, brushless motors with power in the range of 275 to 350 Watts were sought for the implementation of the system. The brushless direct drive hub motor was chosen due to its 80% efficiency, and also it was taken into consideration that the

necessary power is within the operating power of the chosen motor (Figure 5).

Fig. 5 Brushless direct drive hub motor

Fig. 6 The controller shown

Fig. 7 Regulator switching LM2596

2.3.2. Driver Selection

Since the application of this controller is for low speeds, the controller with sensors will be used. The controller to be used is the Gigicloud DC 12V-36V 500W. The controller shown in Figure 6 is ideal for high-power motors. Its speed is controlled by a potentiometer, which gives the feasibility of being controlled by a DAC or a digital-to-analog converter generated by the selected microcontroller.

2.3.3. Battery Selection

After selecting the brushless type electric motor and its respective controller, the necessary batteries were selected to control this system as a whole. In the case of the battery, the minimum and maximum voltage between the controller and the electric motor was taken into account to avoid if a higher capacity battery was chosen; the device could break down or cause an accident. It is also important to analyze the maximum current the motor will consume during its run to carry out the respective analysis. It was estimated that the battery had to guarantee a capacity of at least 3.75Ah. However, for safety purposes and to find commercial batteries, it was decided to take the battery capacity at an exact value of 4Ah. The selected battery will be a "10s2p 18650 battery pack" based on the latter.

2.3.4. Microcontroller Selection

For the selection of the microcontroller, the needs of the controller were taken into consideration, that is, the signals with which the speed of the electric motor must be controlled by means of the controller. In addition, the availability of microcontrollers in the local market was considered. Additionally, the specifications raised in the development of the block diagram raised in the previous section were considered, which resulted in the selection of the ESP32-S2 microcontroller.

2.3.5. Microcontroller Regulator Selection

After determining the controller, the necessary regulation source was selected to power the controller; this source must guarantee the 5 volts necessary for the correct operation of the device; therefore, the selection opted for the LM2596 adjustable switching regulator that is presented in Figure 7.

2.3.6. Selection of Sensors

For the inclination sensor, the MPU6050 accelerometer was selected, which also provides a measurement of the acceleration at which the sensor moves and of the inclination in the 3 ordered axes. This helped in the control part. The aforementioned is desired to guarantee to cut the power to the bicycle when the inclination is greater than a certain angle, which would indicate a fall or dangerous curve. For the measurement of the speed of the system, the GPS NEO-6M module was selected because this module has the ability to measure the position in which it is located by generating longitude and latitude data.

Additionally, it was considered that the system should measure the speed of rotation of the motor wheel. It was decided to implement a tachometer using a Hall effect sensor. For the presentation of data of implemented system, the option of implementing a human-machine interface (HMI) was considered; this selection was made taking into consideration the ease of use of the HMI, as well as the ease of the user to interpret the data which will be presented in it.

2.4. Hardware Design

After selecting the components, the exact hardware was designed to implement the electric bicyclesystem. For this, a new block diagram was made where the selected interconnected modules are represented (Figure 8).

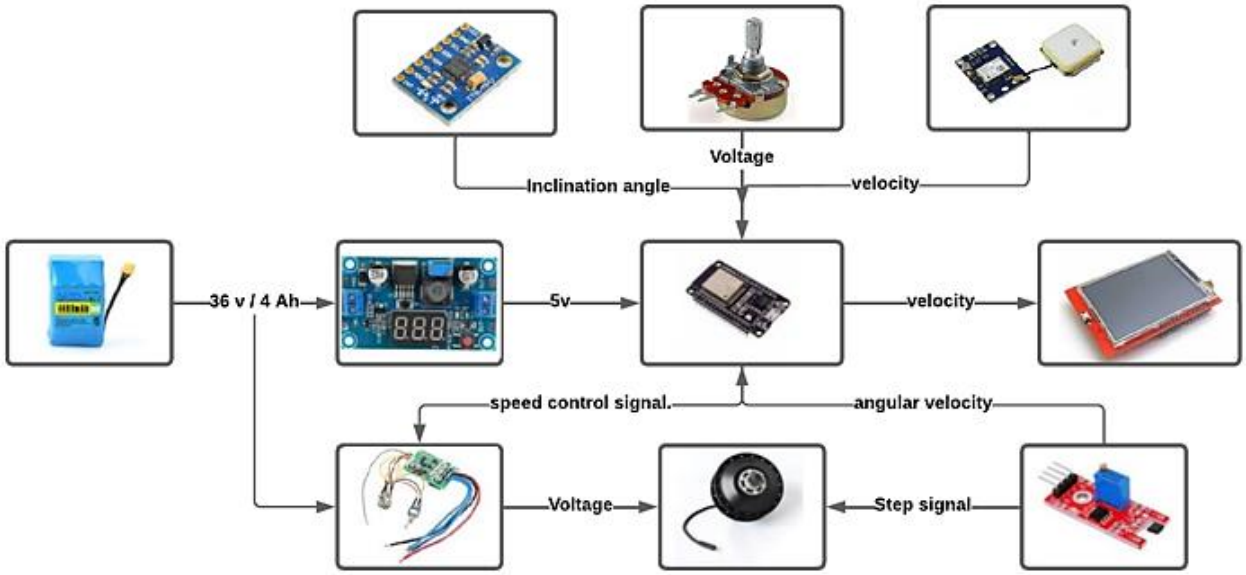

Fig. 8 System block diagram based on components

Figure 8 presents all the selected components in relation to the calculations of necessary power, necessary voltage, control signals, parameter measurement and established regulations.

2.5. Hardware Implementation

The design presented in Fig. 8 was implemented to carry out the tests (Figure 9).

On the other hand, in the power circuit, the selected motor controller was implemented together and connected to the 5200 mAh battery, as shown in Figure 10.

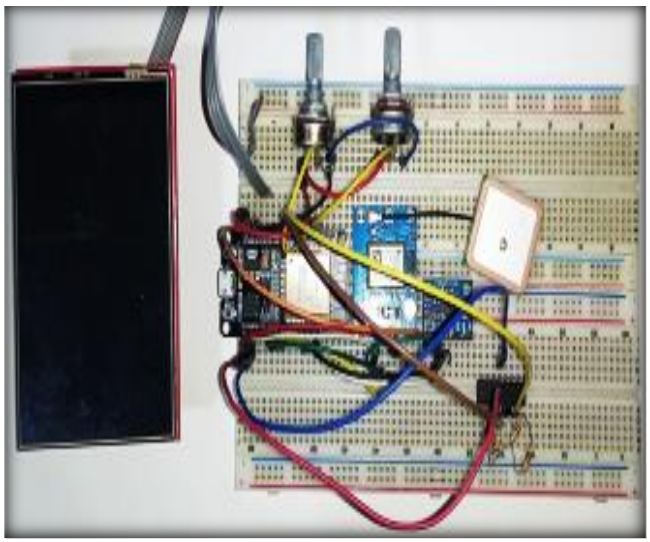

Fig. 9 Implementation of hardware on the breadboard

Fig. 10 Implementation of the controller with the battery

2.6. Mechanical Design

A conventional Lion's brand bicycle was used and represented in the Inventor 2023 software for the mechanical design, as shown in Figure 11. This was used as a baseline.

The bicycle conversion kit developed in this work was implemented for this regular bicycle. Hence, a referential 3D model of the basic used bicycle was obtained to implement the electric bicycle to make the necessary structural modifications for implementing the system. The brushless motor was implemented in the front motor wheel. This representation is shown in Figure 12.

Fig. 11 Baseline regular bicycle

Fig. 13 Bicycle with brushless motor and with implemented control circuit

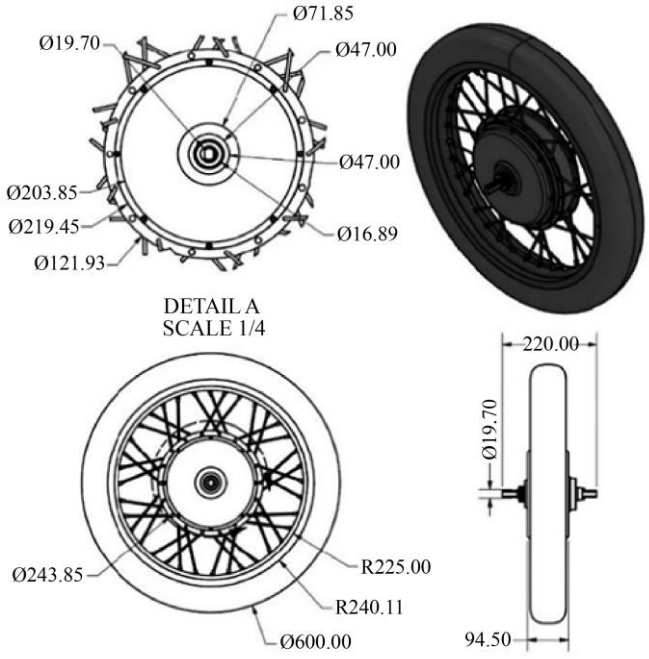

Fig. 12 Brushless motor bicycle wheel

As can be seen in Figure 13, the complete conversion kit fromconventional bicycle to electric bicycle was incorporated. It is from this design that we will start to perform the tests. In this way, we can see the implemented components of the electric bicycle. This referential view helped implement the control and power systems of the whole system. In addition, it will provide an overview of the layout of the most crucial elements of electric bicycle operation. Likewise, the position of the accelerator and brake can be observed, these being crucial elements for the control and handling of the bicycle.

2.7. Firmware Design

After the delimitation of the design components of the electric bicycle, the programming of the embedded microcontroller within the control system was carried out in order to generate the optimal operating conditions during the bicycle journey; these considerations will be programmed following a logic of the closed-loop control processes, using the necessary sensors for feedback and generation of the control signal to activate the system. Likewise, the programming of the TFT screen was carried out in a modular way in order to guarantee better manoeuvrability of the main microcontroller, ESP32-S2.

2.7.1. TFT Screen Programming

Within the programming, or firmware design, of the electric bicycle control system, it was considered the most appropriate way to guarantee that all the resources of the microcontroller focus on the control and monitoring of the control variables of the system was to program the TFT LCD screen in a modular way, that is to say, that it has an intermediary microcontroller in charge of controlling this screen and presenting the information coming from the main microcontroller. This small modification on the initial approach of the screen was made by placing an Arduino Uno development board as the control board for the TFT LCD screen.

The programming of the Arduino Uno in charge of controlling the TFT LCD screen was carried out in the Arduino IDE software. The programming carried out on the microcontroller was carried out in such a way that the main microcontroller sends only one data frame, and these are presented on the TFT LCD screen. The control logic can be seen in Figure 14.

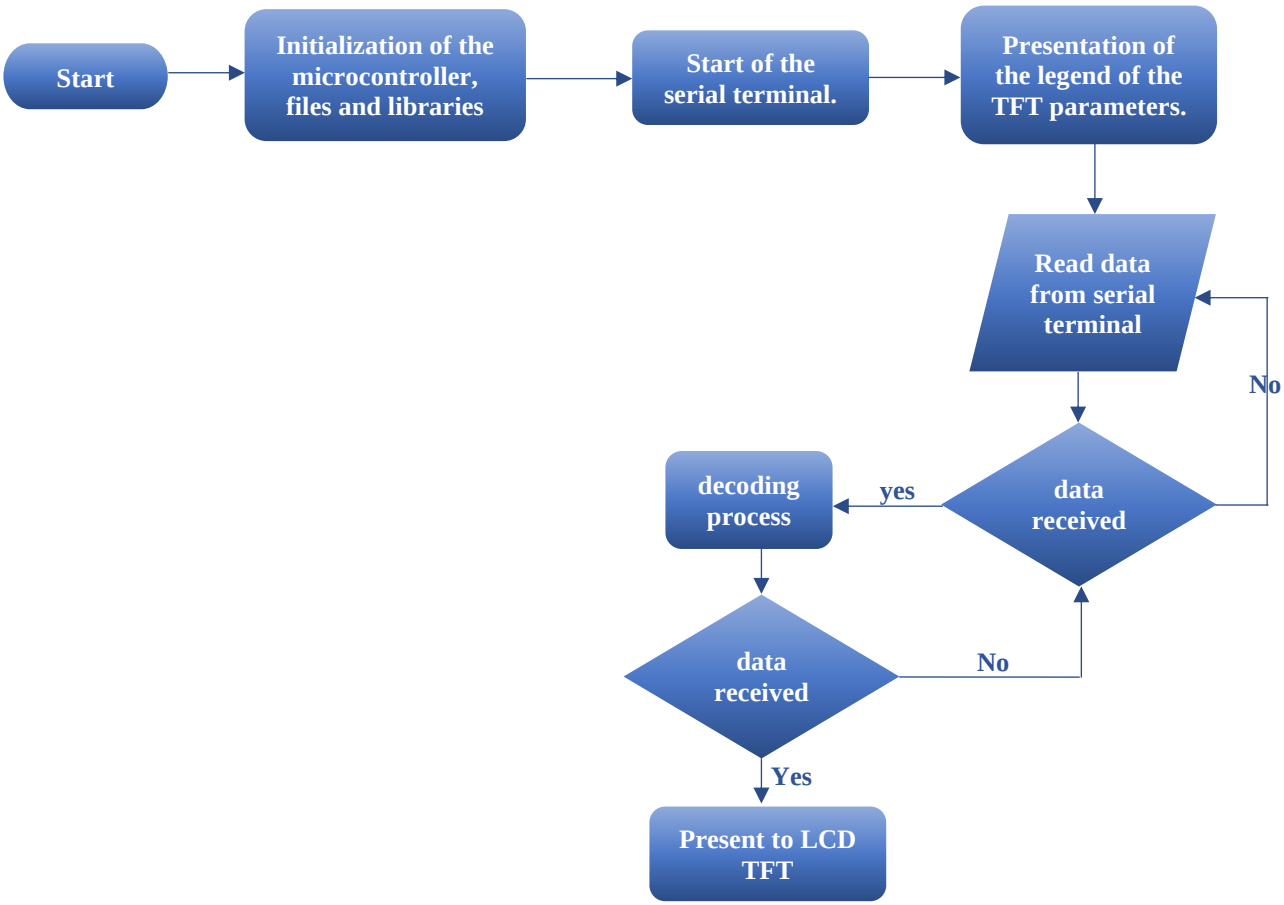

Fig. 14 TFT LCD control flow chart

Fig. 15 Presentation on TFT LCD screen

The inclination, the slope, the state of the motor, the changes, the linear speed and the revolutions per minute can be seen in Figure 15.

2.7.2 Main Microcontroller Programming

Once the programming of the TFT LCD screen was finished, the programming of the main microcontroller, ESP32-S2, was carried out. For this, a previous approach was made of the sequence that the code should follow to be able to perform the necessary measurements to carry out the control of the system implemented in the electric bicycle. For this reason, it was decided to make a flowchart in which the operation of firmware implemented to control the system is explained (Figure 16). The code was made in the Arduino IDE software to work with a familiar and easy-to-manipulate environment.

The necessary modules for configuring the GPS module, MPU6050 module and serial communication wereinitialized. The code for reading the slope and inclination of the MPU6050 was implemented to determine the required angles. The bank angles are extremely important; thus, it was considered that maximum values of the lateral inclination angle should be established to consider that a fall occurred and interrupted the power supply to the motor. Maximum and minimum bank angles are 25° and -25°, respectively—a representation of bank angles is shown in Figure 17.

Likewise, it was considered to carry out a control action onthe slope variation. This is by means of the angle measured by the MPU6050 inclination sensor. Thus, a selection of "gears" produced on the operation of bicycle was generated to supply more power and be able to overcome the effect of slope against it. It should be noted that these gears will be applicable in the assisted driving mode, which the user can enter with the button incorporated into the ESP32-S2.

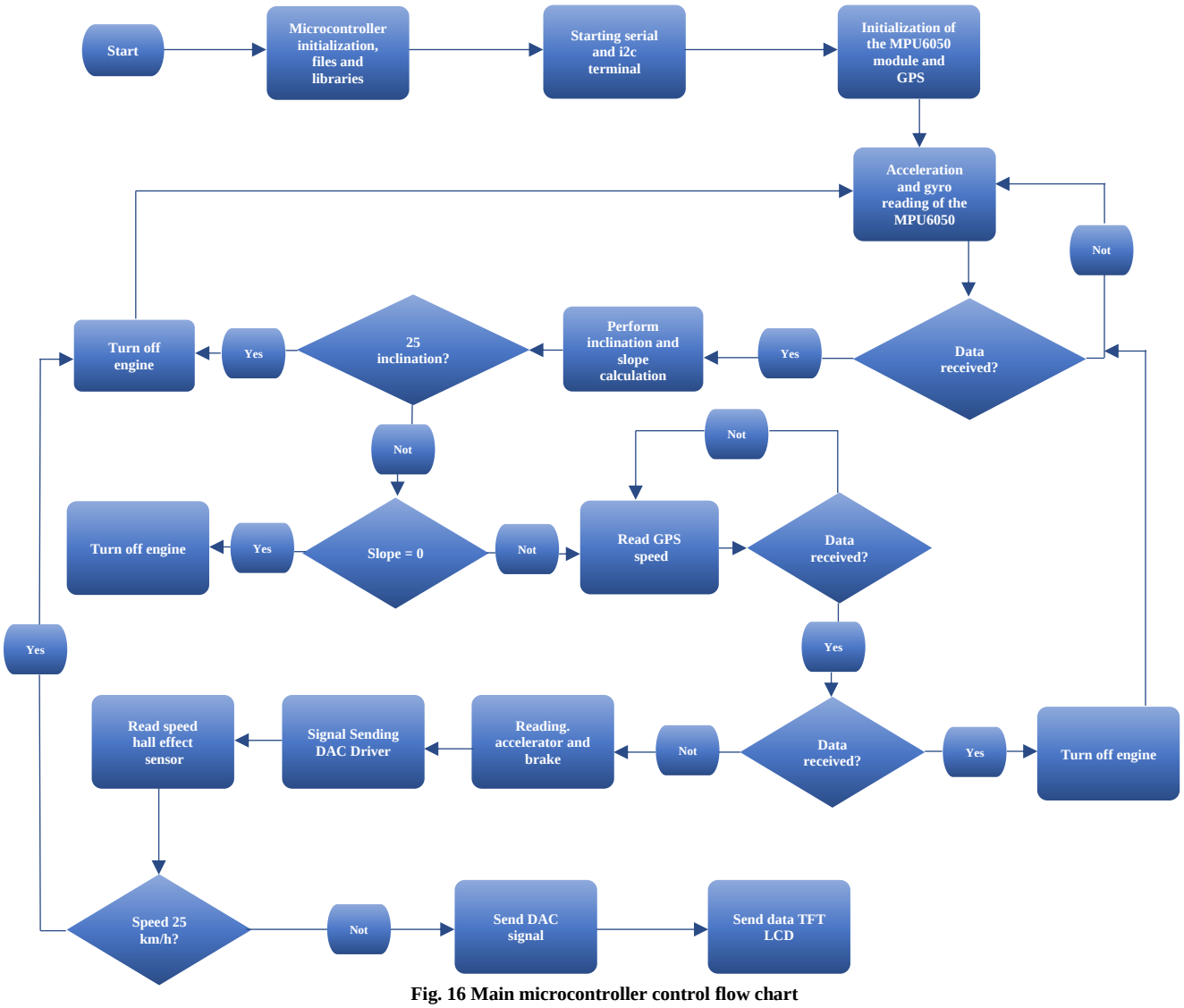

Fig. 16 Main microcontroller control flow chart

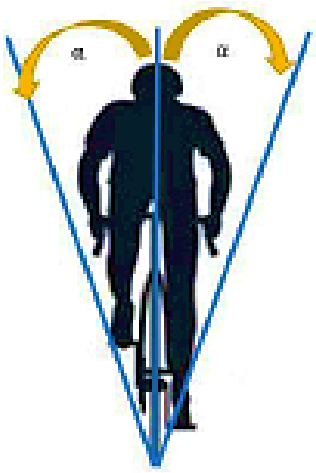

Fig. 17 Bicycle side lean

As observed in Table I, the functionality of up to 5 gears within the assisted operation of the electric bicycle was considered. This will help the user to be able to move easily in environments that have a certain inclination that makes it difficult to climb.

Table 1. Dependence of gears on displacement slope

Inclination (°)	Gear
0°	0
3° > i >= 1°	1
6° > i >= 3°	2
9° > i >= 6°	3
9° >= i	4

2.8. Data Acquisition

For the acquisition of the data required during the tests of the electric bicycle, it was noted that it would

be very difficult to extract the data on the same e-bike because it needs to be in motion to obtain the required data, and the little memory of a microcontroller does not allow extract a minimum required data. Thus, remote data acquisition was chosen thanks to the characteristic of the ESP32 microcontroller that has the bluetooth peripheral. From this, the microcontroller was connected to the HC-05 bluetooth module, and this, in turn, was connected to a computer to use the Arduino IDE Serial Plotter tool.

As shown in Figure 18, the connection of the HC-05 bluetooth receiver with the USB-TTL module can be seen, which transforms the data received by bluetooth to the USB protocol so that the computer recognizes them.

Fig. 18 Bluetooth and USB-TTL modules

2.9. Control Circuit PCB Layout

For PCB design software, there are several options, such as KiCAD, EAGLE, Altium and EasyEDA. Of these options, EasyEDA was used since it is being used in modules and due to its large community of module footprints, it makes it very easy to find the footprints. The routing of tracks was carried out, as shown in Figure 19.

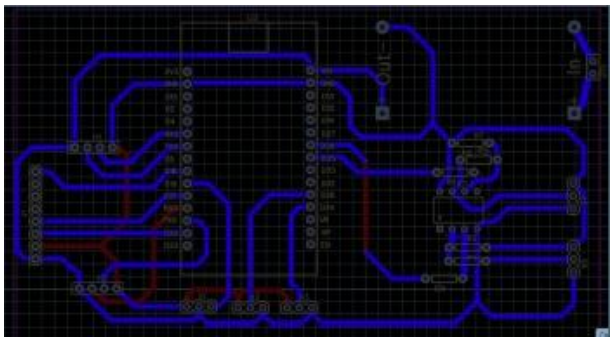

Fig. 19 PCB routing

Figure 20 shows the PCB ready for system implementation and for the respective tests.

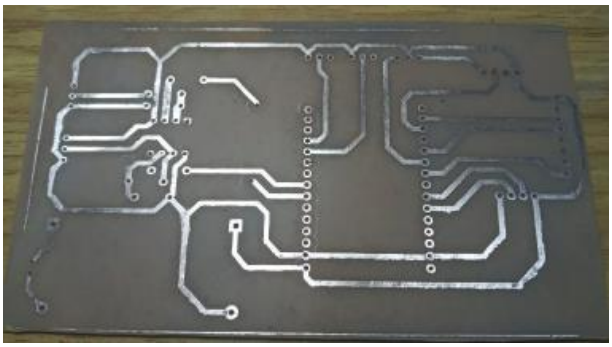

Fig. 20 Control system PCB

3. Results and Discussion

In the design based on the mathematical model, the required torque and the power of the brushless motor were determined for the characteristics of an urban road infrastructure and the requirements of [23] were taken into account, which mentions that the maximum speed of an electric bicycle is 25 km/h. The maximum torque of 24 Nm was obtained. Also, a maximum value of 275 W of maximum power required was obtained. Therefore, selecting an engine with a minimum of such power was necessary. In the market, the power standards of the selected brushless motor are 250 W and 350 W; given this, the 350 W motor was selected.

The control circuit, having previously surface-soldered modules, facilitated PCB design because a multi-layer PCB was formed, resulting in fewer traces. Figure 21 shows the PCB of the control circuit with all the components soldered. In the tests of the interaction of the selected components, the first result was that the LM2596 switching regulator module provided a constant voltage despite the movement and vibrations of the electric bicycle, which is supported by [24, 25, 26]. This allows the ESP32 microcontroller to not be open to possible failures such as resets or false data due to voltage irregularities. In addition, since the microcontroller references the input voltage to read the ADC, this enabled accurate conversion from analog todigital values for the potentiometers. Secondly, the LM2596 regulator, being of the switching type, provides an efficiency of 90%, which surpasses other e-bike controllers in reducing the voltage from the battery to the controller.

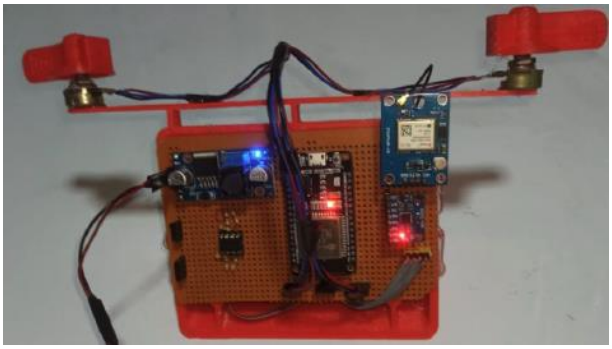

Fig. 21 Electronic bike control PCB

The casing was implemented on the upper part of the bicycle, as shown in Figure 22. It fits precisely on the handlebars of the bicycle.

Fig. 22 Implementation of the control circuit casing

The wiring of the control circuit to the motor and motor controller was placed in areas of non-interference to the user, as shown in Figure 23, considering also what was dictated by [20], which mentions that wiring must not harm the user both when it is moving and when it is not.

Fig. 23 General wiring of electronic bike

The position of the casing allows the user to observe important data easily. In addition, the 3.95-inch screen gives the possibility of displaying a greater amount of data without the need for user manipulations, unlike commercial e-bikes that only provide a single piece of data on their screens.

The electric motor's assistance must be stopped immediately to obtain an optimal design of the electric bicycle in the event of a dangerous malfunction. As explained in the previous sections, it is important to control the motor when there is an accident and, as [16] argues, to be able to turn off the motor automatically to safeguard the integrity of the user. Therefore, the tests are carried out under two contexts. As the first point, the engine's behaviour on a normal route is presented, where the inclinations are typical of the cyclist's route.

This first scenario is carried out under the premise that the person normally moves for his daily route. From this tour, data acquisition of the inclination and the state of the motor's operation was carried out using the Arduino IDE Serial Plotter tool. Figure 24 shows that the inclination α does not exceed the maximum bank angle of 25°, supported by [8]. As explained, during this scenario, it is ensured that the motor works regularly and assists the system's operation.

In Figure 25, we can see the result of the screen of the first scenario. In this, it can be seen that inclination is 1°, a value less than 25°, and due to this, it indicates that the motor status is "ON".

The second scenario is developed under the premise that the person normally moves through his daily route, but at a certainmoment, an accident makes him lean sharply to one of the sides. Like the previous scenario, the data acquisition of the inclination and the state of the motor operation was carried out in the Arduino IDE Serial Plotter tool. In Figure 26, it is observed that the inclination α exceeds the bank angle of 25° maximum supported by [16]. As explained, during this scenario, it is ensured that the engine stops running and assistance to the system is stopped.

Fig. 24 Referential photograph of the first scenario

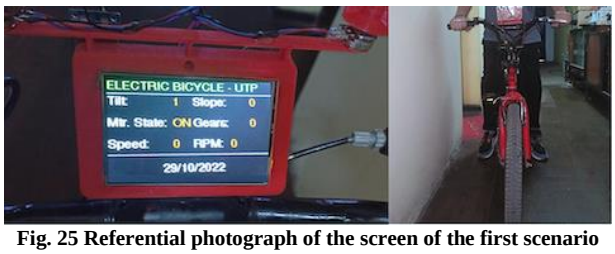

Fig. 25 Referential photograph of the screen of the first scenario

Fig. 26 Referential photograph of the second scenario.

Fig. 27 Referential photograph of the screen of the second scenario.

Fig. 28 Referential photo of the slope of 0°.

Fig. 29 Referential photo of the screen with a slope of 0°.

Figure 27, we can see the result of screen of the second scenario; in this, the inclination is 25°, a value equal to or greater than 25°, and due to this, it indicates that motor status is "OFF". It is important to note that, from those reviewed in state of the art, e-bikes do not usually have fall control.

Figure 28 shows the e-bike moving on a track with a slopeof 0°. During this slope according to Table I, the gear inthis slope is the number 0. Figure 29 shows how the cyclist is informed about the 0° slope scenario, and because it is less than 1° the gear that corresponds to it is 0.

Figure 30 shows the e-bike moving on a track with a slope between 1° and 3°. During this slope according to Table I, the gear in this slope is number 1. Figure 31 shows how the cyclistis informed about the 2° slope scenario, and because it is less than 3° and greater than 1° the gear corresponding to it is 1.

Fig. 30 Referential photo of the slope of 1° to 3°.

Fig. 31 Referential photo of the screen with a slope of 2°.

Fig. 32 Referential photo of the slope of 3° to 6°.

Fig. 33 Referential photo of the screen with a slope of 4°.

Figure 32 shows the e-bike moving on a track with a slope between 3° and 6°. During this slope according to Table I, the gear in this slope is number 2. Figure 33 shows how the cyclist is informed about the 4° slope scenario, and because it is less than 6° and greater than 3° the gear that corresponds to it is 2.

Fig. 34 Referential photo of the slope of 6° to 9°.

Fig. 35 Referential photo of the screen with a slope of 7°.

Figure 34 shows the e-bike moving on a track with a slope between 6° and 9°. During this slope according to Table I, the gear in this slope is number 3. Fig. 35 shows how the cyclist is informed about the 7° slope scenario, and because it is less than 7° and greater than 6° the gear that corresponds to it is 3.

4. Conclusion

In determining and implementing the optimal design to convert a conventional bicycle into a low-cost electric bicycle for urban transportation, the requirements were designed based on the mathematical model of a regular bicycle. From this, it was obtained that the maximum torque requirement is 24 Nm, and the maximum power required of the brushless motor is 275 W. For this reason, a motor of 350W was chosen.

Likewise, the control PCB was obtained by integrating the selected components, which provided a robust and efficient system thanks to its voltage regulator. In addition, in the installation and wiring of the control PCB casing, what is dictated by the European Standard NF EN 15194 was considered. Also, a large screen was installed compared to commercial e-bikes that allow observing all the necessary data for the user. On the other hand, for the efficiency of the proposed design, the European Standard NF EN 15194 was taken as a criterion, so the control was carried out to limit the motor's assistance when reaching the maximum speed.

In addition, the cyclist lean control was performed so that the engine is immediately shut down if the cyclist falls. Likewise, a gear change system was incorporated in the face of different slopes perceived in urban territories

.

It was considered important to compare and analyze commercial screens that provide better visibility against sunlight and have a large size as the screen ofthe present work. In addition, the battery's efficiency can be improved by integrating regenerative braking since this would lengthen the system's autonomy. Together with the gear system proposed in the present investigation, it could further improve the autonomy of the e-bike.

References

[1] Fundacion Transitemos, Situación del Transporte Urbano en Lima y Callao, 2018. [Online]. Available: https://transitemos.org/propuestas/situacion-del-transporte-urbano-en-lima-y-callao/

[2] eBikeChices, Bicicleta eléctrica vs kit de conversion, [Online]. Available: https://www.ebikechoices.com/es/bicicleta-el%C3%A9ctrica-o-kit-de-conversi%C3%B3n/

[3] F. Hoyos, Juan et al., "Investigación, diseño y prototipo de una bicicleta eléctrica y tecnologías emergentes en baterías," *Revista Investigaciones Aplicadas*, vol. 8, no. 1, pp. 60-70, 2014. [Google Scholar] [Publisher Link]

[4] C. Abagnale et al., "Design and Development of an Innovative E-Bike," *Energy Procedia*, vol. 101, no. 9, pp. 774–781, 2016. [CrossRef] [Google Scholar] [Publisher Link]

[5] Jaewon Sung et al., "A study of the Dynamic Characteristics And Required Power Of An Electric Bicycle Equipped with A Semi-Automatic Transmission," *Energy Procedia*, vol. 142, pp. 2057-2064, 2017. [CrossRef] [Google Scholar] [Publisher Link]

[6] Aluri Nishanth, Kumar, Salim, A. Channiwala, "Design and Development of Solar Assisted Electric Cart, 2015. [Online]. Available: https://repository.up.ac.za/handle/2263/49488

[7] Samadhan .S. Avhad, Tushar.P.Tidke, and Nayan .S. Sathe, "Hybrid Electric Bicycle a New Transportation for Future Smart Grid," *SSRG International Journal of Electrical and Electronics Engineering*, vol. 4, no. 6, pp. 15-21, 2017. [CrossRef] [Publisher Link]

[8] Jonathan Weinert, Chaktan Ma, and Christopher Cherry, "The Transition to Electric Bikes in China: History and Key Reasons for Rapid Growth," *Transportation*, vol. 34, pp. 301-318, 2007. [CrossRef] [Google Scholar] [Publisher Link]

[9] Christopher R. Cherry et al., "Dynamics of electric bike ownership and use in Kunming, China," *Transport Policy*, vol. 45, pp. 127-135, 2016. [CrossRef] [Google Scholar] [Publisher Link]

[10] Yinye Yang et al., "Development of an External Rotor V-Shape Permanent Magnet Machine For E-Bike Application," *IEEE Transactions on energy conversion*, vol. 33, no. 4, pp. 1650-1658, 2018. [CrossRef] [Google Scholar] [Publisher Link]

[11] W. Chlebosz, G. Ombach, and J. Junak, "Comparison of Permanent Magnet Brushless Motor with Outer and Inner Rotor Used in E-Bike," *The XIX International conference on electrical machines – ICEM 2010*, 2010. [CrossRef] [Google Scholar] [Publisher Link]

[12] Rohit Tripathi et al., "Modeling and Designing Of E-Bike for Local Use," *Electric Vehicles*, pp. 199-212, 2020. [CrossRef] [Google Scholar] [Publisher Link]

[13] D. S. H. Abhilash et al., "Power Efficient E-Bike with Terrain Adaptive Intelligence," *International Conference On Communication and Electronics Systema (ICCES)*, pp. 1148-1153, 2019. [CrossRef] [Google Scholar] [Publisher Link]

[14] G. R. C. Mouli, P. V. Duijsen, F. Grazian, A. Jamodkar, P. Bauer, and O. Isabella, "Sustainable E-Bike Charging Station that Enables AC, DC and Wireless Charging From Solar Energy," *Energies*, vol. 13, no. 14, 2020. [CrossRef] [Google Scholar] [Publisher Link]

[15] K. Ramesh Kumar, "Modified Mechanical Structure Electric Bike Design Computation and Prototype Model Implementation," *Advances in materials science and engineering*, vol. 2021, 2021. [CrossRef] [Google Scholar] [Publisher Link]

[16] Geethanjali Thejasree, and Ranjith Maniyeri "E-bike System Modeling and Simulation," *IEEE International Conference on Intelligent Systems and Green Technology (ICISGT 2019*), no. 1, pp. 9–14, 2019. [CrossRef] [Google Scholar] [Publisher Link]

[17] Philip M. Gerhart, Andrew L. Gerhart, and John I. Hochstein, *Munson, Young and Okiishi's Fundamentals of Fluid Mechanics*, Wiley, 2016.

[18] Sarah Catherine Walpole et al., "The Weight of Nations: An Estimation of Adult Human Biomass," *BMC Public Health*, vol. 12, no. 1, p. 1, 2012. [CrossRef] [Google Scholar] [Publisher Link]

[19] Alicia Triviño-Cabrera et al., "Design and Implementation of a Cost-Effective Wireless Charger for an Electric Bicycle," *IEEE Access*, vol. 9, pp. 85277-85288, 2021. [CrossRef] [Google Scholar] [Publisher Link]

[20] Carmelina Abagnale et al., "A Dynamic Model for the Performance and Environmental Analysis of an Innovative E-Bike," *Energy Procedia*, vol. 81, pp. 618–627, 2015. [CrossRef] [Google Scholar] [Publisher Link]

[21] Powerdrives, "What is an Electronic speed controller?" [Online]. Available: https://powerdrives.net/blog/what-is-an-esc

[22] Ministerio de Transportes y Comunicaciones, "Decreto Supremo que aprueba el Reglamento de la Ley 30936, Ley que promueve y regula el uso de la bicicleta como medio de transporte sostenible, modifica el Reglamento Nacional de Tránsito, aprobado por Decreto Supremo N 033-2001-MTC." [Online]. Available: https://www.gob.pe/institucion/mtc/normas-legales/633229-012-2020-mtc

[23] European Standards, "ILNAS EN 15194". [Online]. Available: https://www.en-standard.eu/ilnas-en-15194-cycles-electrically-power-assisted-cycles-epac-bicycles/

[24] Sandra M. Castano et al., "Radial Forces and Vibration Analysis in An External-Rotor Switched Reluctance Machine," *IET Electric Power Applications*, vol. 11, no. 2, pp. 252-259, 2017. [CrossRef] [Google Scholar] [Publisher Link]

[25] Chyi-Ren Dow et al., "A Vibration Reduction System For E-Bikes," *IEEE 9th Annual information technology, electronics and mobile communications conference (IEMCON)*, pp. 772-775, 2018. [CrossRef] [Google Scholar] [Publisher Link]

[26] Zachary Bosire Omariba, Lijun Zhang, and Dongbai Sun, "Review of Battery Cell Balancing Methodologies for Optimizing Battery Pack Performance in Electric Vehicles," *IEEE Access*, vol. 7, pp. 129335-129352, 2019. [CrossRef] [Google Scholar] [Publisher Link]

[27] Safwan A. Hamoodi, Ahmed A. Abdullah Al-Karakchi, Ali N. Hamoodi, "Studying Performance Evaluation of Hybrid E-Bike Using Solar Photovoltaic System," *Bulletin of Electrical Engineering and Informatics*, vol. 11, no. 1, pp. 59-67, 2022. [CrossRef] [Google Scholar] [Publisher Link]